Lattice-reduction-aided detection for MIMO-OFDM-CDM communication systems

J. Adeane, M.R.D. Rodrigues and I.J. Wassell

Abstract: Multiple input multiple output-orthogonal frequency division multiplexing-code division multiplexing (MIMO-OFDM-CDM) techniques are considered to improve the link reliability/spectral efficiency of very high data rate communication systems. In particular, lattice-reduction-aided receivers are proposed for MIMO-OFDM-CDM systems. Simulation results show that the proposed receivers significantly outperform the conventional zero-forcing, minimum mean-squared error, or vertical Bell Labs layered space–time receivers without severely compromising system complexity.

1 Introduction

The major challenges in future wireless communication system design are improved link reliability and spectral efficiency. Multiple input multiple output (MIMO) technology has recently become of great interest since it can improve spectral efficiency without sacrificing link reliability [1–3] or improve link reliability without sacrificing spectral efficiency [4–6].

In very high data rate MIMO communication systems, the radio channel introduces severe intersymbol interference (ISI). In this case, single carrier-based MIMO systems require highly complex equalisation techniques. On the other hand, multicarrier-based MIMO systems, for example, MIMO-orthogonal frequency division multiplexing (OFDM), require less complex equalisation techniques because the underlying frequency selective channel is transformed into a set of parallel flat fading channels.

Recently, code division multiplexing (CDM) techniques have been proposed as an alternative to conventional coding techniques to exploit channel time and frequency diversity in OFDM-based systems [7–9]. In this case, consecutive data symbols are spread using orthogonal spreading codes over several OFDM subcarriers and symbols. However, OFDM-CDM suffers from spreading code interference due to loss of spreading code orthogonality in fading channels. The problem is compounded in MIMO-OFDM-CDM since it suffers from both spreading code interference as well as spatial interference. Consequently, efficient detection methods are demanded for MIMO-OFDM-CDM systems.

In this context, a number of linear and nonlinear detection techniques have previously been proposed. Maximum likelihood (ML) detectors are optimal but highly complex. Linear detectors, for example, zero-forcing (ZF) and minimum mean-squared error (MMSE), as well as nonlinear detectors, for example, vertical Bell Labs layered space–time (V-BLAST), are less complex but suboptimal [7–9].

In this article, we propose a novel class of nonlinear detection techniques based on lattice reduction [10–12] for MIMO-OFDM-CDM systems. Lattice-reduction-aided (LRA) receivers achieve nearly optimal performance with low complexity.

2 System model

Figs. 1 and 2 show the block diagrams of an $N \times M$ MIMO-OFDM-CDM communication system, where N and M are the number of transmit and receive antennas, respectively.

At the transmitter, at the nth transmit antenna chain, the transmit data symbols are partitioned into blocks of P transmit data symbols $\boldsymbol{x}_n = [x_n(1), x_n(2), \ldots, x_n(P)]^{\mathrm{T}}$, spread and interleaved. The relation between the blocks of spread symbols $\boldsymbol{s}_n = [s_n(1), s_n(2), \ldots, s_n(P)]^{\mathrm{T}}$ and unspread symbols $\boldsymbol{x}_n = [x_n(1), x_n(2), \ldots, x_n(P)]^{\mathrm{T}}$ can be written as follows

$$\boldsymbol{s}_n = \boldsymbol{C}_P \boldsymbol{x}_n \tag{1}$$

where $\boldsymbol{C}_P$ is the $P \times P$ spreading code transform matrix. For example, the $P \times P$ Hadamard transform matrix is given by

$$\boldsymbol{C}_P = \frac{1}{\sqrt{P}} \begin{bmatrix} \boldsymbol{C}_{P/2} & \boldsymbol{C}_{P/2} \\ \boldsymbol{C}_{P/2} & -\boldsymbol{C}_{P/2} \end{bmatrix}, \quad P = 2^a, \quad a \geq 1 \tag{2}$$

and

$$\boldsymbol{C}_1 = 1 \tag{3}$$

Note that columns of the Hadamard transform matrix correspond to orthogonal spreading code sequences.

Subsequently, N_c interleaved and spread symbols are imposed onto N_c OFDM subcarriers by means of an IFFT, a cyclic prefix is inserted and finally the signal is D/A converted and then upconverted to the desired radio frequency (RF). Note that the duration of the cyclic prefix B is longer than the duration of the impulse response of the radio fading channel L to avoid ISI and intercarrier interference.

At the receiver, at the mth receive antenna chain, the signal is downconverted from the RF, A/D converted, the cyclic prefix is removed, and the N_c receive symbols are

doi:10.1049/iet-com:20050640

Paper first received 6th December 2005 and in revised form 9th August 2006

The authors are with the Laboratory for Communication Engineering, Department of Engineering, University of Cambridge, 15 JJ Thomson Avenue, Cambridge CB3 0FD, UK

E-mail: ja316@cam.ac.uk

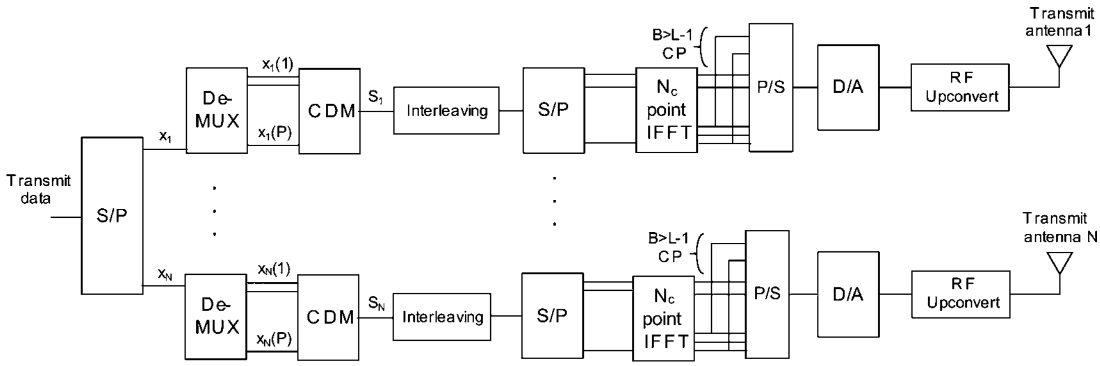

Fig. 1 *MIMO-OFDM-CDM transmitter*

recovered from the N_c OFDM subcarriers by means of an FFT.

Subsequently, the receive symbols are de-interleaved and partitioned onto blocks of P receive symbols $\boldsymbol{y}_m = [y_m(1), y_m(2), \ldots, y_m(P)]^{\mathrm{T}}$. Detection is based on the observation of the various blocks of P receive symbols of the receive antenna chains. It is assumed that the receiver maintains perfect channel state information.

We note that it is possible to relate the input to the mth demultiplexer at the receiver, $\boldsymbol{y}_m = [y_m(1),\ y_m(2), \ldots, y_m(P)]^{\mathrm{T}}$ to the input to the various demultiplexers at the transmitter, $\boldsymbol{x}_n = [x_n(1),\ x_n(2), \ldots x_n(P)]^{\mathrm{T}}$, $n = 1, \ldots, N$, as follows

$$\boldsymbol{y}_m = \sum_{n=1}^{N} \boldsymbol{H}_{mn} \boldsymbol{C}_P \boldsymbol{x}_n + \boldsymbol{w}_m \tag{4}$$

where $\boldsymbol{H}_{mn}$ is a $P \times P$ diagonal matrix containing the channel frequency responses between the nth transmit antenna and mth receive antenna on the P subcarriers on which the transmit data elements corresponding to $\boldsymbol{x}_n$ have been transmitted, and $\boldsymbol{w}_m = [w_m(1),\ w_m(2), \ldots, w_m(P)]^{\mathrm{T}}$ is the noise at the mth receive antenna on the P subcarriers. We assume that the additive noise random variables are uncorrelated circularly symmetric complex Gaussian.

Finally, it is possible to relate the input of the various demultiplexers at the receiver $\boldsymbol{y} = [\boldsymbol{y}_1^{\mathrm{T}}, \boldsymbol{y}_2^{\mathrm{T}}, \ldots, \boldsymbol{y}_M^{\mathrm{T}}]^{\mathrm{T}}$ to the input of the various demultiplexers at the transmitter $\boldsymbol{x} = [\boldsymbol{x}_1^{\mathrm{T}}, \boldsymbol{x}_2^{\mathrm{T}}, \ldots, \boldsymbol{x}_N^{\mathrm{T}} \boldsymbol{y}_M^{\mathrm{T}}]^{\mathrm{T}}$ as follows

$$\boldsymbol{y} = \boldsymbol{\mathcal{H}} \boldsymbol{x} + \boldsymbol{w} \tag{5}$$

where $\boldsymbol{\mathcal{H}}$ is a $(M\ \ P) \times (N\ \ P)$ matrix given by

$$\boldsymbol{\mathcal{H}} = \begin{bmatrix} \boldsymbol{H}_{11}\boldsymbol{C}_P & \cdots & \boldsymbol{H}_{1N}\boldsymbol{C}_P \\ \vdots & \ddots & \vdots \\ \boldsymbol{H}_{M1}\boldsymbol{C}_P & \ldots & \boldsymbol{H}_{MN}\boldsymbol{C}_P \end{bmatrix} \tag{6}$$

and $\boldsymbol{w} = [\boldsymbol{w}_1^{\mathrm{T}}, \boldsymbol{w}_2^{\mathrm{T}}, \ldots, \boldsymbol{w}_M^{\mathrm{T}}]^{\mathrm{T}}$. We define the matrix $\boldsymbol{\mathcal{H}}$ as the MIMO-OFDM-CDM channel matrix.

3 LRA detection for MIMO-OFDM-CDM communication systems

3.1 Conventional detection

3.1.1 Linear detection: In conventional linear detection, the receive equalised signal $\boldsymbol{y}^{\mathrm{eq}}$ is initially obtained from the receive unequalised signal $\boldsymbol{y}$ as follows

$$\boldsymbol{y}^{\mathrm{eq}} = \boldsymbol{G}\boldsymbol{y} = \boldsymbol{G}\boldsymbol{\mathcal{H}}\boldsymbol{x} + \boldsymbol{G}\boldsymbol{w} \tag{7}$$

where $\boldsymbol{G}$ is the matrix equaliser. The estimate of the transmit data signal is subsequently obtained as follows

$$\hat{\boldsymbol{x}} = \mathcal{Q}(\boldsymbol{y}^{\mathrm{eq}}) \tag{8}$$

where $\mathcal{Q}(.)$ denotes the quantisation operation. For ZF equalisation, $\boldsymbol{G} = \boldsymbol{\mathcal{H}}^{\dagger}$, where $\boldsymbol{\mathcal{H}}^{\dagger} = (\boldsymbol{\mathcal{H}}^{\mathrm{H}}\boldsymbol{\mathcal{H}})^{-1}\boldsymbol{\mathcal{H}}^{\mathrm{H}}$ is the pseudoinverse of the extended MIMO-OFDM-CDM channel matrix $\boldsymbol{\mathcal{H}}$. The ZF criterion suffers from noise enhance-ment especially if $\boldsymbol{\mathcal{H}}$ is rank-deficient or ill-conditioned. For MMSE equalisation, $\boldsymbol{G} = \sigma_x^2 \boldsymbol{\mathcal{H}}^{\mathrm{H}}(\boldsymbol{\mathcal{H}}\boldsymbol{\mathcal{H}}^{\mathrm{H}} + \sigma_w^2 \boldsymbol{I}_{MP})^{-1}$, where σ_x^2 is the transmit data power, σ_w^2 the noise power and $\boldsymbol{I}_{MP}$ the $(M\ \ P) \times (M\ \ P)$ identity matrix. The MMSE criterion does not suffer from noise enhancement.

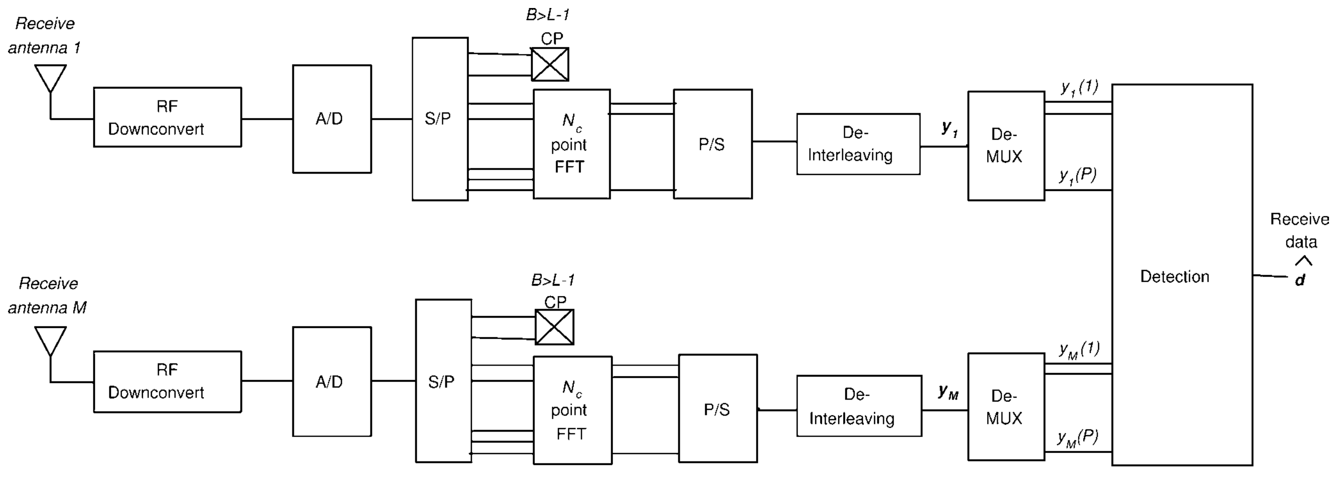

Fig. 2 *MIMO-OFDM-CDM receiver*

3.1.2 V-BLAST detection: Golden *et al.* [13] proposed the V-BLAST space–time architecture that achieves a very high spectral efficiency and a good trade-off between complexity and performance. The V-BLAST space–time architecture uses an ordered serial nulling plus cancellation detection technique which progresses from the strongest to the weakest data stream. This results in the maximisation of the minimum post-detection signal-to-noise-ratio of the data streams. Ha and Lee [9] proposed the V-BLAST detection technique for MIMO-OFDM-CDM.

3.2 LRA detection

Yao and Wornell [10] first proposed LRA receivers for 2×2 MIMO systems. Berenguer *et al.* [12] later extended the LRA receiver technique to general $N \times M$ MIMO-OFDM systems, where $M \geq N$. In this article, we propose LRA receivers for MIMO-OFDM-CDM communication systems.

In LRA techniques, the channel matrix $\mathcal{H}$ is seen as the generator matrix of some lattice. Moreover, the channel matrix columns are seen as the generator basis of the same lattice. Let us consider for simplicity, the two-dimensional case to illustrate the motivation behind LRA techniques. Fig. 3 shows that if the angle between the basis vectors $\boldsymbol{h}_1$ and $\boldsymbol{h}_2$ corresponding to the columns of the generator matrix $\mathcal{H}$ is very narrow (i.e. the vectors are highly correlated), even a small amount of noise can cause a receive symbol to fall out of its own decision region into another decision region thereby causing the decoder to make a wrong decision. The objective of LRA techniques is to determine a change of basis $\boldsymbol{F}$, which transforms the generator matrix of the lattice, $\mathcal{H}$, into another generator matrix of the same lattice, $\mathcal{H}' = \mathcal{H}\mathbf{F}$, such that the decision regions for a specific equaliser and decoder are optimised, that is such that the basis vectors are closer to orthogonal. The equalising and decoding operations are subsequently performed in the new basis rather than in the original basis. The decoded symbols are finally transformed from the new to the original basis.

Consider a vector of transmit data symbols represented by $\boldsymbol{x}$ in the original basis with elements in $\mathbb{Z}_C$, the set of complex integers, and represented by $\boldsymbol{x}_{\text{new}} = \boldsymbol{F}^{-1}\boldsymbol{x}$ in the new basis also with elements in $\mathbb{Z}_C$. Consider also the vector of receive symbols represented by $\boldsymbol{y}$ in the original basis and represented by $\boldsymbol{y}_{\text{new}} = \boldsymbol{F}^{-1}\boldsymbol{y}$ in the new basis. In particular

$$\begin{aligned} \boldsymbol{y}_{\text{new}} &= \boldsymbol{F}^{-1}\boldsymbol{y} = \boldsymbol{F}^{-1}\mathcal{H}(\boldsymbol{F}\boldsymbol{F}^{-1})\boldsymbol{x} + \boldsymbol{F}^{-1}\boldsymbol{w} \\ &= \boldsymbol{F}^{-1}\mathcal{H}\boldsymbol{F}\boldsymbol{x}_{\text{new}} + \boldsymbol{F}^{-1}\boldsymbol{w} \end{aligned} \quad (9)$$

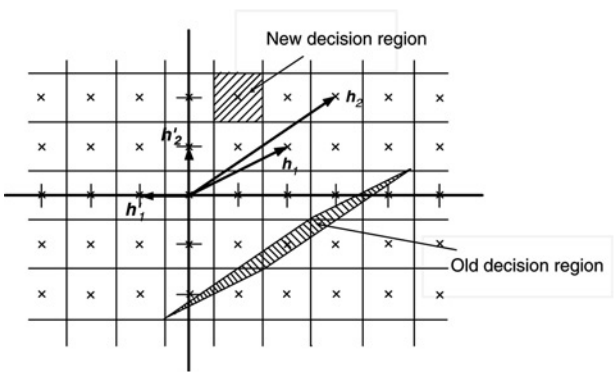

Fig. 3 *Original basis, new basis and decision regions*

Now, conventional LRA uses the equaliser matrix $\boldsymbol{G} = (\boldsymbol{F}^{-1}\mathcal{H}\boldsymbol{F})^{\dagger}$ to equalise the signal in the new basis. Consequently, the equalised symbols in the new basis are given by

$$\boldsymbol{y}_{\text{new}}^{\text{eq}} = \boldsymbol{G}\boldsymbol{y}_{\text{new}} = \boldsymbol{G}\boldsymbol{F}^{-1}\mathcal{H}\boldsymbol{F}\boldsymbol{x}_{\text{new}} + \boldsymbol{G}\boldsymbol{F}^{-1}\boldsymbol{w} \quad (10)$$

$$= \boldsymbol{x}_{new} + \boldsymbol{G}\boldsymbol{F}^{-1}\boldsymbol{w} \quad (11)$$

and the decoded symbols in the new basis are given by

$$\hat{\boldsymbol{x}}_{\text{new}} = \mathcal{Q}(\boldsymbol{y}_{\text{new}}^{\text{eq}}) \quad (12)$$

Here, the quantisation operation $\mathcal{Q}(.)$ corresponds to a rounding operation because the symbols in the lattice are in $\mathbb{Z}_C$. The decoded symbols are finally transformed from the new to the original basis producing the estimate $\hat{\boldsymbol{x}} = \boldsymbol{F}\hat{\boldsymbol{x}}_{\text{new}}$.

Lattice theory requires the original points in the constellation to consist of symbols in $\mathbb{Z}_{\mathbb{C}}$ (i.e. to consist of contiguous integers and contain the origin). However, standard Q-QAM constellations (where $\Re\{x\} \in \{-\sqrt{Q}+1, \ldots, \sqrt{Q}-1\}$ and $\Im\{x\} \in \{-\sqrt{Q}+1, \ldots, \sqrt{Q}-1\}$) neither consist of contiguous integers nor contain the origin.

One way to overcome this problem is by shifting the original constellation points by $\boldsymbol{l} = [1+i, \ldots, 1+i]^{\text{T}}$ and scaling the resulting points by $1/2$ [12].

Note that in the absence of noise, the vector of receive symbols $\boldsymbol{y}'$ given a vector of shifted and scaled transmit symbols $\boldsymbol{x}'$ is

$$\boldsymbol{y}' = \mathcal{H}\boldsymbol{x}' = \mathcal{H}\frac{1}{2}[\boldsymbol{x} + \boldsymbol{l}] \quad (13)$$

which is equivalent to

$$\boldsymbol{y}' = \frac{1}{2}\boldsymbol{y} + \frac{1}{2}\mathcal{H}\boldsymbol{l} \quad (14)$$

Consequently, the required shifting and scaling operations can be directly incorporated by manipulation of the vector of receive symbols $\boldsymbol{y}$.

To summarise, an LRA receiver first implements the scale, shift, change to new basis operations and then performs equalisation in the new basis, that is

$$\boldsymbol{y}_{\text{new}}^{\text{eq}} = \underbrace{(\boldsymbol{F}^{-1}\mathcal{H}\boldsymbol{F})^{\dagger}}_{\text{equalise in new basis}} \underbrace{\boldsymbol{F}^{-1}}_{\text{change basis}} \underbrace{\frac{1}{2}}_{\text{scale}} [\boldsymbol{y} + \underbrace{\mathcal{H}\boldsymbol{l}}_{\text{shift}}] \quad (15)$$

which, when $N = M$ and the channel matrix is full rank, simplifies to

$$\boldsymbol{y}_{\text{new}}^{\text{eq}} = \boldsymbol{F}^{-1}\mathcal{H}^{-1}\frac{1}{2}(\boldsymbol{y} + \mathcal{H}\boldsymbol{l}) \quad (16)$$

An LRA receiver finally implements the rounding, change to original basis and undo scale and shift operations, that is

$$\hat{\boldsymbol{x}} = 2\boldsymbol{F}\mathcal{Q}(\boldsymbol{y}_{\text{new}}^{\text{eq}}) - \boldsymbol{l} \quad (17)$$

The operations of an hybrid LRA-V-BLAST receiver are equivalent to those of the conventional LRA receiver just described. However, detection in the new basis follows the usual V-BLAST ordered serial nulling and cancellation operations [1, 13].

3.3 Basis reduction algorithm

This section describes the basis reduction algorithm for MIMO-OFDM-CDM systems. Specifically, we consider the problem of determining a change of basis $\boldsymbol{F}$ to transform the original basis vectors for the lattice, $\boldsymbol{h}_1, \boldsymbol{h}_2, \ldots, \boldsymbol{h}_N$, into another basis vectors for the same lattice $\boldsymbol{h}_1', \boldsymbol{h}_2', \ldots, \boldsymbol{h}_{N'}$, which are closer to being mutually orthogonal. This basis reduction problem uses some ideas behind Gram-Schmidt (GS) orthogonalisation.

For simplicity, we will initially illustrate the concept for the two-dimensional scenario where the columns of $\mathcal{H}$, that is, $\boldsymbol{h}_1$ and $\boldsymbol{h}_2$, are the basis vectors of the lattice. We will initially discuss an ideal GS orthogonalisation and weakly reduced GS orthogonalisation, and finally lattice reduction.

3.3.1 Ideal GS orthogonalisation:

The GS process is a method of orthogonalising a set of vectors in an inner product space. The GS process determines from a set of linearly independent vectors, another set of mutually orthogonal vectors that span the same subspace as the original vectors.

In the two-dimensional case, the ideal GS process works as follows

$$\boldsymbol{h}_1' = \boldsymbol{h}_1 \tag{18}$$

$$\boldsymbol{h}_2' = \boldsymbol{h}_2 - \mu \boldsymbol{h}_1 \tag{19}$$

where $\mu = \langle \boldsymbol{h}_1, \boldsymbol{h}_2 \rangle / \langle \boldsymbol{h}_1, \boldsymbol{h}_1 \rangle$ is the GS coefficient and $\langle \boldsymbol{a}, \boldsymbol{b} \rangle = \boldsymbol{a}^{\mathrm{H}} \boldsymbol{b}$. Note that this operation can potentially change the lattice associated with the original basis vectors $\boldsymbol{h}_1$ and $\boldsymbol{h}_2$ since μ may not belong to $\mathbb{Z}_{\mathbb{C}}$. Thus, this method cannot be directly used in lattice reduction.

3.3.2 Weakly reduced GS orthogonalisation:

The weakly reduced GS orthogonalisation process is identical to the ideal GS orthogonalisation method with the additional constraint that the GS coefficient belongs to $\mathbb{Z}_{\mathbb{C}}$. Note that this method will not change the lattice associated with the original basis vectors $\boldsymbol{h}_1$ and $\boldsymbol{h}_2$. However, the vectors of the reduced basis are only close to orthogonal. Thus, this method can be in principle used in lattice reduction.

The weakly reduced GS orthogonalisation rounds the real and imaginary parts of the ideal GS coefficients separately, that is $\mu' = \lfloor \mu \rceil$. In the two-dimensional case, assuming that $\|\boldsymbol{h}_2\| > \|\boldsymbol{h}_1\|$, we have the possibility of reducing $\boldsymbol{h}_2$ with respect to $\boldsymbol{h}_1$

$$\boldsymbol{h}_2 = \boldsymbol{h}_2 - \mu' \boldsymbol{h}_1 \tag{20}$$

Further reduction will occur if $\mu' < 0$, that is, $|\Re\{\langle \boldsymbol{h}_1, \boldsymbol{h}_2 \rangle\}| > (1/2)\|\boldsymbol{h}_1\|^2$ or $|\Im\{\langle \boldsymbol{h}_1, \boldsymbol{h}_2 \rangle\}| > (1/2)\|\boldsymbol{h}_1\|^2$. The algorithm repeats iteratively until no more reduction is possible. An example of a pair of new bases produced by this basis reduction algorithm is shown in Fig. 3.

3.3.3 Lattice reduction:

Lenstra, Lenstra and Lovasz (LLL) proposed an algorithm to reduce the lattice basis $\boldsymbol{h}_1, \boldsymbol{h}_2, \ldots, \boldsymbol{h}_N$ in polynomial time [14][1]. A detailed explanation on the complexity of the algorithm can be found in ([14]. Briefly, if C is the bit-length of the coefficients of the input basis and D is the dimension of the lattice, the total number of arithmetic operations performed is $O(D^4 \log C)$. This has since been improved to $O(D^3 \log C)$ using integer and floating point number of length $O(D + \log C)$ [15]). For a given δ, $1/4 < \delta < 1$, the LLL reduction algorithm modifies the original basis $\boldsymbol{h}_1, \ldots, \boldsymbol{h}_N$ continuously using an iterative process similar to the weakly reduced GS orthogonalisation so that the following conditions are satisfied (21) and (22)

$$\mu_{n,m} \leq \frac{1}{2} \quad \text{for} \quad 1 \leq m < n \leq N \tag{21}$$

$$\delta \|\hat{\boldsymbol{h}}_{k-1}\|^2 > \|\hat{\boldsymbol{h}}_k + \mu_{k,k-1} \hat{\boldsymbol{h}}_{k-1}\|^2 \tag{22}$$

where the GS vectors $\hat{\boldsymbol{h}}_1, \ldots, \hat{\boldsymbol{h}}_N$ are equal to

$$\hat{\boldsymbol{h}}_1 = \boldsymbol{h}_1$$

$$\hat{\boldsymbol{h}}_n = \boldsymbol{h}_n - \sum_{m=1}^{n-1} \mu_{n,m} \hat{\boldsymbol{h}}_m \quad \text{for } n = 2, \ldots, N \tag{23}$$

and the GS coefficients, are equal to

$$\mu_{n,m} = \frac{\langle \hat{\boldsymbol{h}}_m, \boldsymbol{h}_n \rangle}{\langle \hat{\boldsymbol{h}}_m, \hat{\boldsymbol{h}}_m \rangle} \tag{24}$$

Fig. 4 shows an implementation of the LLL algorithm. Note that the vectors $\{\boldsymbol{h}_1, \ldots, \boldsymbol{h}_k\}$, the GS vectors $\{\hat{\boldsymbol{h}}_1, \ldots, \hat{\boldsymbol{h}}_k\}$, and the corresponding GS coefficients $\mu_{n,m}$ are continuously updated. Note also that the iterative reduction process is carried out by the exchange of adjacent vectors $\boldsymbol{h}_{k-1}$ and $\boldsymbol{h}_k$ until conditions (21) and (22) are satisfied. The algorithm stops when further reduction is not possible. In this case, the reduced basis $\{\boldsymbol{h}_1', \ldots, \boldsymbol{h}_k'\}$ is taken to be equal to updated $\{\boldsymbol{h}_1, \ldots, \boldsymbol{h}_k\}$.

Finally, the parameter δ controls both the speed of convergence of the algorithm as well as the degree of orthogonality of the reduced basis. In particular, the higher the value of δ, the higher the degree of orthogonality of the reduced basis. However, the higher the value of δ, the slower the speed of convergence of the algorithm. The value $\delta = 0.7$ constitutes a good tradeoff, so will be used subsequently.

4 Results and discussion

Simulations are conducted for MIMO-OFDM-CDM systems with the following parameters: $N = M = 2$ and $N = M = 4$ antennas, number of OFDM subcarriers $N_c = 64$, cyclic prefix length $B = 16$, Hadamard spreading codes with length $P = 4$ and 8, a block interleaver with interleaving depth $\pi = N_c/P$ and QPSK and 16-QAM modulation. The radio fading channel is composed of three independent and resolvable Rayleigh faded paths with delays 0, 0.4 and 0.9 µs, and average powers 1, 0.3 and 0.1, respectively. Bit-error-rate (BER) results are averaged over 50 independent channel realisations for each SNR.

Figs. 5–8 show that the two proposed LRA receivers significantly outperform both the conventional linear ZF and MMSE receivers as well as the ZF and MMSE V-BLAST receivers. For example, in Fig. 5, the conventional LRA receiver outperforms ZF and MMSE receivers by more than 15 and 10 dB, respectively, at a BER $= 10^{-3}$. The conventional LRA receiver also outperforms the conventional MMSE V-BLAST receiver by 4 dB at a BER $= 10^{-3}$. In addition, the performance of LRA-V-BLAST is better than conventional LRA by 1 dB at high SNR, however, there is an additional complexity penalty associated with the BLAST ordering process.

LRA receivers are also very effective for MIMO-OFDM-CDM systems with arbitrary spreading code length. Note that longer spreading code lengths can potentially increase the (system) diversity order but at the same time also increases the (system) interference [7, 8]. Figs. 5 and 6 demonstrate that LRA receivers exhibit

Input: Lattice basis $\boldsymbol{h}_1 = \mathcal{H}[:,1], ..., \boldsymbol{h}_N = \mathcal{H}[:,N] \in \mathbb{C}^N$, $\frac{1}{4} < \delta < 1$

$k = 2$

while $k \leq N$ **do**

for $n = k-1, ..., 1$ **do**

$\boldsymbol{h}_k = \boldsymbol{h}_k - \lfloor \mu_{k,n} \rceil \boldsymbol{h}_n$;

end for

Compute $\hat{\boldsymbol{h}}_k$ as in (23)

if $\delta \|\hat{\boldsymbol{h}}_{k-1}\|^2 > \|\hat{\boldsymbol{h}}_k + \mu_{k,k-1}\hat{\boldsymbol{h}}_{k-1}\|^2$ **then**

$\boldsymbol{h}_{k-1} \leftrightarrow \boldsymbol{h}_k$; % exchange

$k = \max(k-1, 2)$

else $k = k+1$

end while

$\boldsymbol{h}'_u = \boldsymbol{h}_u$, for $u = 1, \ldots, N$ % final results

Output: Reduced lattice basis $\mathcal{H}' = [\boldsymbol{h}'_1, ..., \boldsymbol{h}'_N]$ and $\boldsymbol{F}$ defined as $\mathcal{H}' = \mathcal{H}\boldsymbol{F}$

Fig. 4 *LRA lattice-reduction algorithm*

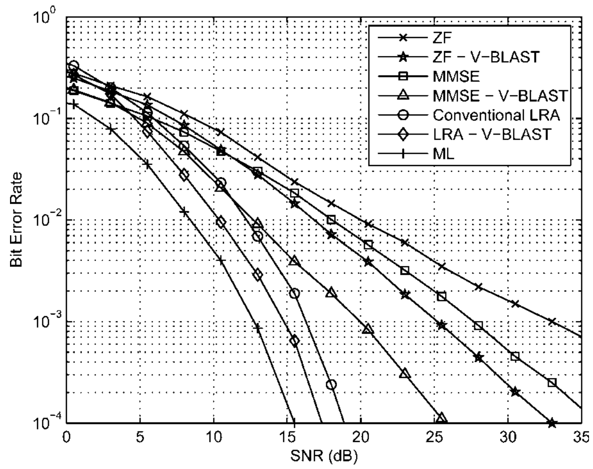

Fig. 5 *BER performance of 2 × 2 MIMO-OFDM-CDM systems with P = 4, QPSK modulation*

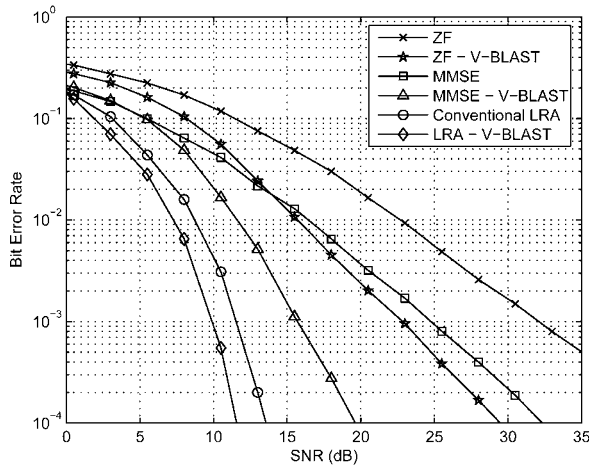

Fig. 7 *BER performance of 4 × 4 MIMO-OFDM-CDM systems with P = 4, QPSK modulation*

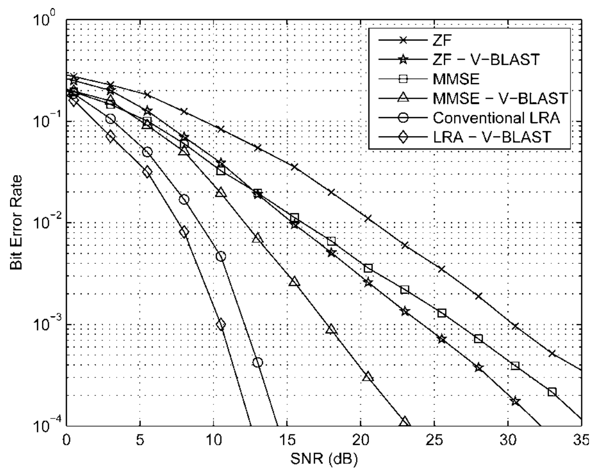

Fig. 6 *BER performance of 2 × 2 MIMO-OFDM-CDM systems with P = 8, QPSK modulation*

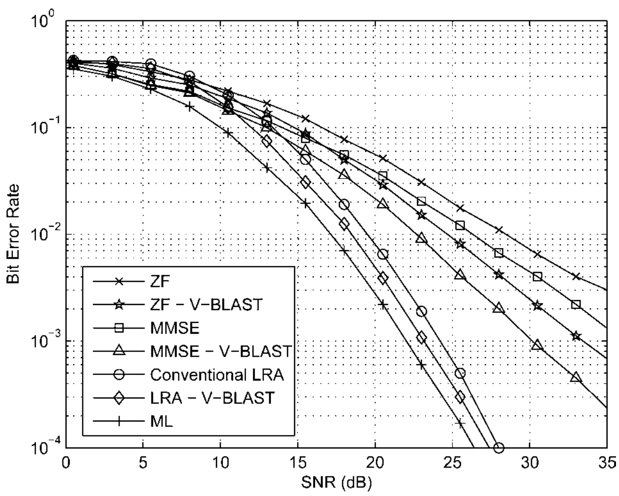

Fig. 8 *BER performance of 2 × 2 MIMO-OFDM-CDM systems with P = 4, 16-QAM modulation*

good BER performance both for $P=4$ and 8. Fig. 5 also shows that the performance of the proposed LRA receivers is close to that of the ML receiver (Note that the ML performance curve is not shown in MIMO-OFDM-CDM systems with a large number of transmit/receive antennas, a large spreading code length or a high constellation order because of excessive simulation time). In particular, the slope of the BER against. SNR curves indicate that the diversity order of LRA receivers is significantly higher than that of ZF, MMSE or V-BLAST receivers, and identical to that of the ML receiver.

LRA receivers are also effective for MIMO-OFDM-CDM systems with arbitrary numbers of transmit and receive antennas. Note that a higher number of transmit and receive antennas also increase the system diversity order but again it also increases spatial interference. However, Figs. 5 and 7 demonstrate that LRA receivers significantly outperform conventional receivers both for systems with $N=M=2$ as well as systems with $N=M=4$.

In addition, LRA receivers also exhibit very good performance for MIMO-OFDM-CDM systems based on different constellations (Figs. 5 and 8). In particular, Yao and Wornell [10] show that the performance of an LRA receiver approaches that of an ML receiver as the constellation order increases, or, as the ratio between the internal points and the boundary points of the constellation increases.

LRA receivers are particularly appropriate for MIMO-OFDM-CDM systems in the presence of slow fading channels. In a slowly varying channel, the calculated reduced basis is valid for a number of consecutive OFDM symbols, which reduces the computational load. This results in LRA receivers with similar complexity to conventional linear receivers, since the bulk of the complexity of LRA receivers is associated with the basis reduction operation.

To conclude, we note that LRA-based receivers are very promising for MIMO-OFDM-CDM systems. In particular, LRA receivers considerably outperform conventional receivers in systems characterised by a high number of transmit/receive antennas, high spreading code length and high constellation order, yet with low complexity when compared with the ML receiver. In addition, Wubben *et al.* [11] show that LRA receivers perform very well in the presence of antenna correlation when the performance of conventional and V-BLAST receivers are poor. Since LRA receivers use basis vectors which are closer to orthogonal, there is less correlation between the columns of $\mathcal{H}'$ when compared to that which is present in the original $\mathcal{H}$ and therefore the LRA receivers perform much better than the linear receivers in correlated channel. Therefore LRA is an attractive method to improve the BER performance when the channel correlation is high.

5 Acknowledgment

The authors would like to thank Inaki Berenguer for valuable discussions.

6 References

1 Foschini, G.J.: 'Layered space–time architecture for wireless communication in fading environment when using multi-element antennas', *Bell Syst. Tech. J.*, 1996, **1**, pp. 41–59

2 Foschini, G.J., and Gans, M.J.: 'On limits of wireless communications in a fading environment when using multiple antennas', *Wirel. Pers. Commun.*, 1998, **6**, pp. 311–355

3 Telatar, I.E.: 'Capacity of multiantenna Gaussian channels', *Eur. Trans. Commun.*, 1999, **10**, pp. 585–595

4 Alamouti, S.M.: 'A simple transmitter diversity scheme for wireless communications', *IEEE J. Sel. Areas Commun.*, 1998, **16**, pp. 1451–1458

5 Tarokh, V., Seshadri, N., and Calderbank, A.R.: 'Space–time codes for high data rate wireless communication: performance criterion and code construction', *IEEE Trans. Inf. Theory*, 1998, **44**, pp. 744–765

6 Tarokh, V., Jafarkhani, H., and Calderbank, A.R.: 'Space–time block codes from orthogonal designs', *IEEE Trans. Inf. Theory*, 1999, **45**, pp. 1456–1467

7 Kaiser, S.: 'Trade-off between channel coding and spreading in multi-carrier CDMA systems'. IEEE Int. Symp. on Spread Spectrum Techniques and Applications, Mainz, Germany, September 1996, vol. 3, pp. 1366–1370

8 Kaiser, S.: 'OFDM code-division multiplexing in fading channels', *IEEE Trans. Commun.*, 2002, **50**, pp. 1266–1273

9 Ha, K., and Lee, K.B.: 'OFDM-CDM with V-BLAST detection and its extension to MIMO systems'. Proc. IEEE Vehicular Technology Conf. Spring, Orlando, Florida, April 2003, vol. 1, pp. 764–768

10 Yao, H., and Wornell, G.W.: 'Lattice-reduction-aided detectors for MIMO communication systems'. Proc. IEEE Global Telecommunications Conf., Taipai, Taiwan, November 2002, vol. 1, pp. 424–428

11 Wubben, D., Kuhn, V., and Kammeyer, K.-D.: 'On the robustness of lattice-reduction aided detectors in correlated MIMO systems'. Proc. IEEE Vehicular Technology Conf., Los Angles, USA, September 2004, vol. 5, pp. 3639– 3643

12 Berenguer, I., Adeane, J., Wassell, I.J., and Wang, X.: 'Lattice-reduction-aided receivers for MIMO-OFDM in spatial multiplexing systems'. Proc. IEEE Int. Symp. on Personal, Indoor and Mobile Radio Communications, Barcelona, Spain, September 2004, vol. 2, pp. 1516–1521

13 Golden, G.D., Foschini, G.J., Valenzuela, R.A., and Wolniansky, P.W.: 'Detection algorithm and initial laboratory results using the V-BLAST space–time communication architecture', *Electron. Lett.*, 1999, **35**, pp. 14–15

14 Lovasz, L.: 'An algorithmic theory of numbers, graphs, and convexity' (SIAM, Philadelphia, PA, 1986)

15 Schnorr, C.-P., and Koy, H.: 'Segment LLL-reduction with floating point orthogonalization'. Int. Conf. Cryptography and Lattices (CaLC). (Springer, 2001), Lecture Notes in Computer Science, vol. 2146, pp. 81–96